

IMPLICATIONS OF THE X-RAY VARIABILITY FOR THE MASS OF MCG–6-30-15

MICHAEL A. NOWAK¹ AND JAMES CHIANG¹

Submitted 1999 June 23; Accepted 2000 January 12

ABSTRACT

The bright Seyfert 1 galaxy MCG–6-30-15 shows large variability on a variety of time scales. We study the $\lesssim 3$ day time scale variability using a set of simultaneous archival observations that were obtained from *RXTE* and the *Advanced Satellite for Cosmology and Astrophysics* (*ASCA*). The *RXTE* observations span nearly 10^6 sec and indicate that the X-ray Fourier Power Spectral Density has an rms variability of 16%, is flat from approximately 10^{-6} – 10^{-5} Hz, and then steepens into a power law $\propto f^{-\alpha}$ with $\alpha \gtrsim 1$. A further steepening to $\alpha \approx 2$ occurs between 10^{-4} – 10^{-3} Hz. The shape and rms amplitude are comparable to what has been observed in NGC 5548 and Cyg X-1, albeit with break frequencies that differ by a factor of 10^{-2} and 10^4 , respectively. If the break frequencies are indicative of the central black hole mass, then this mass may be as low as $10^6 M_{\odot}$. An upper limit of ~ 2 ks for the relative lag between the 0.5–2 keV *ASCA* band compared to the 8–15 keV *RXTE* band was also found. Again by analogy with NGC 5548 and Cyg X-1, this limit is consistent with a relatively low central black hole mass.

Subject headings: galaxies: individual (MCG–6-30-15) — galaxies: Seyfert — X-rays: galaxies

1. INTRODUCTION

The type 1 Seyfert galaxy MCG–6-30-15 has in recent years been the subject of intense study owing to the discovery by the *Advanced Satellite for Cosmology and Astrophysics* (*ASCA*) of a resolved, broad iron $K\alpha$ fluorescent line in its hard X-ray spectrum (Tanaka et al. 1995). The shape of the line is consistent with a gravitationally and Doppler shifted emission line which originates from near the inner edge of an accretion disk around a black hole. In the X-rays, MCG–6-30-15 is also one of the brighter and more variable type 1 Seyferts. It is therefore hoped that by examining the correlated variability between the ionizing X-ray continuum and various components of the Fe $K\alpha$ line, one can obtain a size scale for the system and thence a mass for the black hole (Reynolds et al. 1999). This requires, however, that the various components of the line be spectrally resolved on time scales shorter than the intrinsic response time scale of the line-emitting material.

At present, *ASCA*, *BeppoSAX*, and *Chandra* are the only X-ray telescopes with the spectral resolution to measure fluxes in different line components separately. Unfortunately, the integration times ($\gtrsim 10$ ks) required to obtain this resolution are longer than the light travel time across the inner edge of an accretion disk around a $10^8 M_{\odot}$ Schwarzschild black hole. Furthermore, the fits to the iron line appear to require a Kerr geometry (although see Reynolds & Begelman 1997) in order to explain the broad red wing of the line and the lack of significant emission blueward of 6.4 keV, thus making the relevant time scales even shorter. Nonetheless, over longer time scales, *ASCA* has measured significant variability in the shape of the MCG–6-30-15 Fe $K\alpha$ line (Iwasawa et al. 1996).

Time-resolved spectral investigations (Iwasawa et al. 1996; Iwasawa et al. 1999) suggest that the broad and narrow components of the iron line are correlated differently with the flux state depending on the time scale investigated. For integrations $\gtrsim 10^4$ s, the narrow component varies with the continuum flux whilst the broad component appears to be anti-correlated. In contrast, on shorter time scales the broad component responds immediately to flux changes whilst the narrow component re-

mains constant. Iwasawa et al. (1999) suggest that multiple, localized X-ray flares occur on the disk surface near the inner edge and illuminate only a relatively small region of the disk. These small regions make contributions to narrow ranges in line redshift and thus produce very complex temporal behavior.

In support of this interpretation, Iwasawa et al. (1999) consider the iron line associated with a very short, bright flare from MCG–6-30-15 observed during 1997 August by *ASCA* (see Fig. 1). The line was very redshifted and had little or no emission blueward of 6 keV. Its shape was consistent with having originated entirely from a small region at $r \simeq 5$ GM/c² on the approaching side of the disk. The flare lasted about 4 ks, which is also approximately the orbital period at this radius for a $10^7 M_{\odot}$ black hole. In order for the line not to be significantly more smeared by the orbital motion, Iwasawa et al. (1999) estimate a black hole mass of $\sim 2 \times 10^8 M_{\odot}$. Alternatively, they suggest that a much lower mass is possible if all the line emission arises from $r < 5$ GM/c².

A major complication that a high-mass model faces is the large amplitude and rapid X-ray variability of MCG–6-30-15 (Fig. 1). In particular, during the performance verification phase of *ASCA*, Reynolds et al. (1995) noted that the 0.5–10 keV flux increased by a factor 1.5 over 100 s, i.e., the dynamical time scale at the inner disk edge surrounding a maximal Kerr, $2 \times 10^6 M_{\odot}$ black hole. Typically one expects the bulk of the X-ray variability to occur on dynamical time scales or longer. It is clearly important to determine whether this variability represented a rare, rapid event or if such time scales are truly characteristic of the behavior of MCG–6-30-15.

One might expect that characteristic time scales should scale with the mass of the central object (see, e.g., the discussions of McHardy 1988 and Edelson & Nandra 1999); therefore, in this work we try to gauge the size of the system and the mass of the black hole in MCG–6-30-15 by studying its characteristic X-ray variability properties in comparison to other black hole systems such as Cyg X-1 and NGC 5548. For the high-frequency variability analysis, we use the 1997 August simultaneous *ASCA/Rossi X-ray Timing Explorer* (*RXTE*) observation discussed by Iwasawa et al. (1999) (see also Lee et al. 1998).

¹JILA, University of Colorado, Campus Box 440, Boulder, CO 80309-0440, USA; mnowak@rocinate.colorado.edu, chiangj@panza.colorado.edu

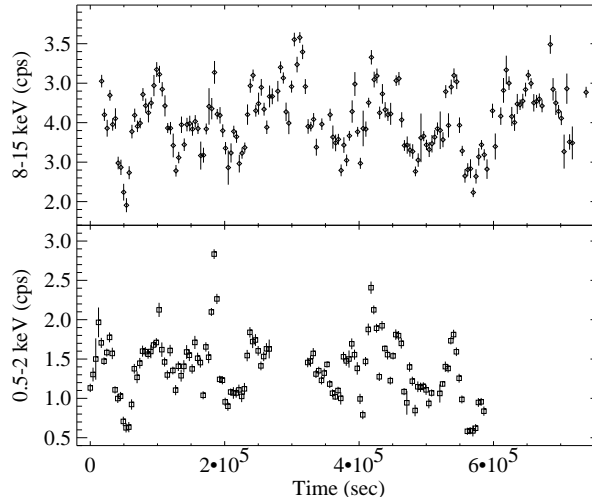


FIG. 1.— The *RXTE* 8–15 keV band (top) and the *ASCA* 0.5–2 keV band (bottom) lightcurves, in 4096 s timebins. These data have been obtained from the archival 1997 August simultaneous *ASCA/RXTE* observation (Lee et al. 1998).

In our analysis we screen the *ASCA* data as outlined by Brandt et al. (1996), except that we use the more stringent criteria of 7 GeV/c for the rigidity and an elevation angle of 10° . Data from both SIS detectors are combined into a single lightcurve. For the *RXTE* data, we use screening criteria and analysis techniques appropriate for faint sources, as we have previously discussed in Chiang et al. (2000). Specifically, we only analyze top layer data from proportional counter units 0, 1, and 2.

2. POWER SPECTRA

MCG–6-30-15 is detected by the *All Sky Monitor (ASM)*; Levine et al. 1996) on *RXTE* with a mean count rate of 0.44 cps in the 1.3–12.2 keV band. Currently, there is a 0.1 cps uncertainty in the zero level offset, as well as comparable magnitude systematic time-dependent variations due to, for example, the solar angular position relative to the source (Remillard 1999, priv. comm.). Assessing the very low frequency ($f \lesssim 10^{-6}$ Hz) X-ray variability of MCG–6-30-15 is therefore problematic. Efforts are currently underway, however, to revise the *ASM* data reduction process in order to minimize such systematic effects (Remillard 1999, priv. comm.); therefore, an ultra-low frequency variability study of MCG–6-30-15 in principle will be feasible in the near future.

We are able, however, to investigate the high-frequency power spectral density (PSD) of MCG–6-30-15 by using the *RXTE* 8–15 keV and the *ASCA* 0.5–2 keV lightcurves binned on 4096 sec time scales. Both lightcurves contain data gaps, especially on the orbital time scale of ≈ 5 ks due to blockage by the Earth and passage through the South Atlantic Anomaly. We therefore use the techniques of Lomb (1976) and Scargle (1982) to calculate the PSD, and we only consider frequencies $f \lesssim 10^{-4}$ Hz (evenly sampled in intervals of the inverse of the observation duration). Higher time resolution lightcurves showed excess power on the ≈ 5 ks orbital time scale. The results, binned over the greater of four contiguous frequency bins or logarithmically over $f \rightarrow 1.15 f$, are presented in Fig. 2. Here we use a one-sided normalization where integrating over positive frequencies yields the total mean square variability relative to the squared mean for the particular lightcurve being analyzed. The *ASCA* lightcurve shows 28% rms variability, whereas the *RXTE* lightcurve shows 16% rms variability. Both

PSD have comparable shapes, i.e., flat from $\approx 10^{-6}$ – 10^{-5} Hz and slightly steeper than f^{-1} at higher frequencies.

We have fit a broken power law to the data, assuming error bars equal to the average PSD value divided by the square root of the number of frequency bins averaged over. Although such error estimates are only valid for averages made from independent frequency bins (which is not strictly true for the Lomb-Scargle periodogram; Scargle 1982), this should provide a rough estimate, especially as the lightcurves are nearly evenly sampled. The best fit PSD slopes are -1.3 ± 0.2 for the *PCA* and -1.6 ± 0.3 for *ASCA* (errors are $\Delta\chi^2 = 2.7$). The break frequencies are found to be $(8 \pm 3) \times 10^{-6}$ Hz for the *PCA*, and $(1.5 \pm 0.5) \times 10^{-5}$ Hz for *ASCA*. These break frequencies are consistent with the value found by McHardy, Papadakis & Uttley (1998).

At frequencies $> 5 \times 10^{-4}$ Hz there are enough contiguous data segments to be able to calculate the PSDs using standard FFT methods (Nowak et al. 1999, and extensive references therein). In Fig. 2 we show the calculated, background and noise-subtracted, PSD for the 1.8–3.6 keV and 8–15 keV *RXTE* bands. Below $\approx 2 \times 10^{-3}$ Hz, where signal to noise is greatest, both PSDs are consistent with being $\propto f^{-2 \pm 0.3}$ and having 6% rms variability. From the generated background lightcurves, we estimate that background fluctuations contribute at most 1.5% and 2% rms variability, respectively, to these PSDs at $< 2 \times 10^{-3}$ Hz. As the PSDs of the background lightcurves tend to be slightly steeper than f^{-2} , there may be some trend for background fluctuations to steepen the observed high-frequency PSDs, and, in fact, Yaqoob (1997) find a slightly flatter ($\propto f^{-1.4}$) high-frequency PSD for MCG–6-30-15.

3. TIME DELAYS

In order to examine time delays between the low energy *ASCA* lightcurve and the high energy *RXTE* lightcurve, we use the Z-transformed Discrete Cross-Correlation Function (ZDCF) of Alexander (1997), which is based upon the DCF method of Edelson & Krolik (1988). Auto-correlation functions can also be computed by this procedure, and we note that PSD derived from autocorrelations calculated via the ZDCF yield identical results to those presented in Fig. 2. We use the Monte

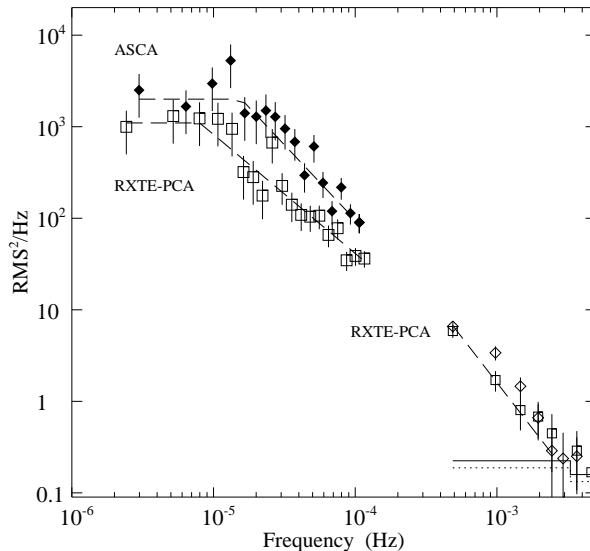


FIG. 2.— PSD constructed from *ASCA* 0.5–2 keV (filled diamonds), *RXTE* 1.8–3.6 keV (open diamonds), and *RXTE* 8–15 keV (open squares) lightcurves. Dashed lines show the broken power law fits discussed in the text and an f^{-2} power law. Background and noise have been subtracted from the high-frequency 1.8–3.6 keV and 8–15 keV *RXTE* PSD, with the residual noise levels shown as a dotted and solid line, respectively.

Carlo methods described by Peterson et al. (1998) to assess the significance of any uncertainties due to flux measurement errors as well as uneven or incomplete sampling.

We have previously applied these methods to a simultaneous *Extreme Ultraviolet Explorer (EUVE)/ASCA/RXTE* observation of NGC 5548 (Chiang et al. 2000), where we found evidence for the low energy *ASCA* band leading the high energy *RXTE* band by 5 ks. The results for the MCG–6-30-15 data are shown in Fig. 3, for which we have used lightcurves binned at 512 s resolution. A positive delay indicates that the *RXTE* light curve lags the *ASCA* light curve. Due to the ambiguities associated with interpreting cross-correlation results, particularly for such small delays, we considered three different measures of the “lag”. For each Monte Carlo trial, we estimate the characteristic lag by (1) fitting a parabola to the ZDCF values to find the location of the peak, (2) computing the centroid of the ZDCF over positive values bracketing the maximum value, and (3) using the location of the actual maximum value of the ZDCF. In all three cases, our simulations yield evidence for a positive lag at various degrees of significance: $\tau_{\text{fit}} = 0.9 \pm 0.7$ ks, $\tau_{\text{centroid}} = 0.9 \pm 1.3$ ks, $\tau_{\text{max}} = 0.4^{+1.9}_{-1.2}$ (90% C.L.). Although the fitted peak estimate is consistent with a positive lag, both the centroid and ZDCF-maximum estimates are formally consistent with zero giving an upper limit of $\tau \lesssim 2$ ks.

At high Fourier frequency, we have used the 1.8–3.6 keV and 8–15 keV *RXTE* lightcurves discussed above to search for frequency-dependent time lags using standard FFT techniques. (A complete discussion of such methods, including calculation of error bars, is presented in Nowak et al. 1999 and references therein). No significant time delays were found, and the $1\text{-}\sigma$ upper limits were 50–100 s in the 5×10^{-4} – 2×10^{-3} Hz range. Note that there were an insufficient number of uninterrupted, strictly simultaneous *ASCA/RXTE* lightcurves to allow calculation of their relative time delays via direct FFT methods.

4. DISCUSSION

The MCG–6-30-15 PSD breaks to being $\propto f^{-1}$ at $\approx 10^{-5}$ Hz, and then breaks to being approximately $\propto f^{-2}$ between 10^{-4} –

10^{-3} Hz. This is to be compared to the Cyg X-1 PSD which has a comparable rms amplitude and shape, and has a set of PSD breaks at frequencies between 0.03–0.3 Hz and 1–10 Hz (Nowak et al. 1999, and references therein). The black hole mass in Cyg X-1 is estimated to be $10 M_{\odot}$ (Herrero et al. 1995); therefore, if these break frequencies scale with mass, then the central black hole mass of MCG–6-30-15 could be as low as $10^6 M_{\odot}$. NGC 5548, which is believed to have a central black hole mass of $10^8 M_{\odot}$ (Done & Krolik 1996; Chiang & Murray 1996; Peterson & Wandel 1999), shows a similar PSD with break frequencies at $\approx 6 \times 10^{-8}$ Hz and between 3×10^{-7} – 3×10^{-6} Hz (Chiang et al. 2000). Again, if the break frequencies scale with mass, then the central black hole mass for MCG–6-30-15 could be several orders of magnitude lower than that for NGC 5548.

To date, the most carefully studied X-ray PSD for any AGN is that for NGC 3516 (Edelson & Nandra 1999). (See also McHardy, Papadakis & Uttley 1998 who present preliminary results for a number of AGN, including MCG–6-30-15.) For NGC 3516 the PSD was seen to break from nearly flat at $\lesssim 3 \times 10^{-7}$ Hz, and then gradually steepen into an $f^{-1.74}$ power law up to frequencies as high as $\approx 10^{-3}$ Hz. NGC 3516 is seen to be intermediate between NGC 5548 and MCG–6-30-15. Based upon these measurements (and upon other factors, such as the source luminosity), Edelson & Nandra (1999) argue for a black hole mass in the range of 10^7 – $10^8 M_{\odot}$, i.e., intermediate to the masses of NGC 5548 and MCG–6-30-15 discussed above.

The *RXTE/ASCA* lag upper limit for MCG–6-30-15 is also intermediate between the observed X-ray lags for Cyg X-1 (Miyamoto et al. 1988; Nowak et al. 1999) and NGC 5548 (Chiang et al. 2000). The time lag observed in NGC 5548, effectively measured on the f^{-2} portion of its PSD, is 5 ks. Time lags on the flat portion of the NGC 5548 PSD could be considerably longer (Chiang et al. 2000). Near the PSD break from flat to f^{-1} , the X-ray time lags in Cyg X-1 are ≈ 0.1 s, whilst on the f^{-2} portion of the PSD the X-ray time lags are 10^{-3} – 10^{-2} s. The MCG–6-30-15 time lags may cover a similar dynamic range

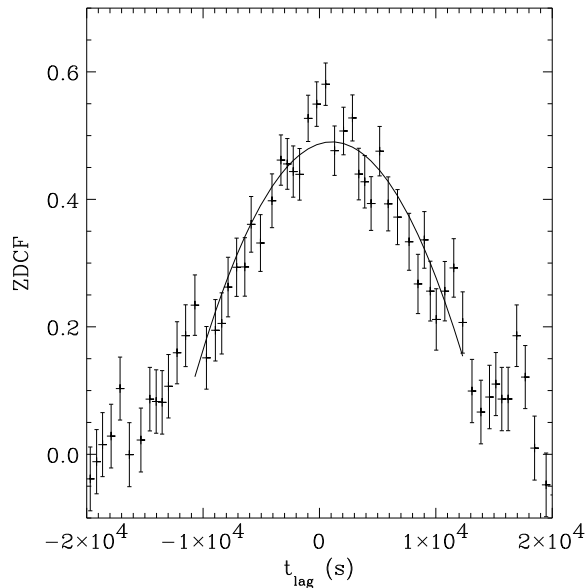


FIG. 3.— Z-transformed discrete correlation function (ZDCF) of the SIS, 0.5-2 keV lightcurve relative to the 8–15 keV *RXTE-PCA* lightcurve (512 s time bins). The solid line is a parabola fit to the ZDCF values. Monte Carlo simulations of these data yield an upper-limit on the *RXTE* time lag of 2.2 ks (90% Confidence Level).

from < 2 ks (overall lag) to < 100 s (high frequency lag²).

If the characteristic variability and lag times are indicative of mass, then a mass as low as $10^6 M_{\odot}$ may be required for the central black hole of MCG–6-30-15. Assuming a bolometric luminosity of 4×10^{43} ergs s^{-1} (Reynolds et al. 1997), this would imply that MCG–6-30-15 is emitting at 30% of its Eddington rate, which is large but still plausible. A relatively low central black hole mass would make the large amplitude, rapid variability reported by Reynolds et al. (1995) much easier to understand, whereas a mass as large as the $2 \times 10^8 M_{\odot}$, the upper end discussed by Iwasawa et al. (1999), seems very unlikely. The $\lesssim 100$ s lags seen at high frequency then likely provide an upper limit to the Compton diffusion time scale (see the discussion of Nowak et al. 1999). These time scales are problematic for future hopes of simultaneously temporally and spectrally resolving the iron $K\alpha$ line in this system with *Constellation-X* as it will require ≈ 1 ks integration times to study the line profile of MCG–6-30-15 (Young & Reynolds 2000).

A 30% Eddington luminosity indicates that it is worthwhile to search for ultra-low frequency ($f \lesssim 10^{-6}$ Hz) variability in excess of $\approx 3\%$ rms, that is, above an extrapolation of the flat part of the *ASCA* and *RXTE-PCA* PSDs. ‘Very high state’, i.e., $\gtrsim \mathcal{O}(30\% L_{\text{Edd}})$, galactic black hole candidates can show PSDs that are flat below $\approx 10^{-2}$ Hz, are approximately proportional to f^{-2} PSD between $\approx 10^{-2}$ – 10^{-1} Hz, are flat again between $\approx 10^{-1}$ –1 Hz, and then break into an f^{-2} PSD at higher frequencies. (Specifically, see Fig. 4b of Miyamoto et al. 1991, which shows a ‘very high state’ PSD of GX339–4.) The low frequency portion of the ‘very high state’ PSD has no simple analogy in the (usually observed) low/hard state of Cyg X-1,

where ultra-low frequency noise is typically associated with dipping activity due to obscuration by the accretion stream (Angelini, White & Stella 1994). Previous models, for example, have associated ‘very high state’ low-frequency variability with fluctuations of a viscously unstable α -disk (Nowak 1994, and references therein).

This highlights the major caveat that needs to be mentioned; we do not know the average PSD shape nor the scaling of the break frequencies as a function of fractional Eddington luminosity in either galactic black hole candidates or AGN. This is an especially important consideration as the mass estimates discussed above imply a large range of Eddington luminosity ratios. Considering all the evidence for rapid variability and extremely short time lags in MCG–6-30-15 discussed above, however, a low mass for MCG–6-30-15 seems to us very compelling. With the advent of the *X-ray Multiple Mirror (XMM)* mission, which has large effective area and is capable of extremely long, uninterrupted observations, these analyses will become more detailed for NGC 5548 and MCG–6-30-15, and will allow one to develop a statistical sample of numerous other AGN.

We thank R. Remillard for generating an *ASM* lightcurve of MCG–6-30-15, and O. Blaes, K. Pottschmidt, N. Murray, and J. Wilms for useful conversations. This work has been financed by NASA Grants NAG5-4731, NAG5-7723, and NAG5-6337. This research has made use of data obtained through the High Energy Astrophysics Science Archive Research Center Online Service, provided by the NASA/Goddard Space Flight Center.

²Although the low energy band here differed from the *ASCA* band, if the time lags scale logarithmically with energy (Nowak et al. 1999 and references therein) we would have expected the lag with respect to the *ASCA* band to be approximately a factor of 2 greater.

REFERENCES

- Alexander, T., 1997, in *Astronomical Time Series*, ed. D. Maoz, et al., (Netherlands: Kluwer Academic Press), 163
- Angelini, L., White, N. E., & Stella, L., 1994, in *New Horizon of X-Ray Astronomy*, ed. F. Makino, T. Ohashi, (Tokyo: Universal Academy Press), 429
- Brandt, W. N., Fabian, A. C., Dotani, T., Nagase, F., Inoue, H., Kotani, T., & Segawa, Y., 1996, *MNRAS*, 283, 1071
- Chiang, J., & Murray, N., 1996, *ApJ*, 466, 704
- Chiang, J., Reynolds, C. S., Blaes, O., Nowak, M. A., Murray, N., Madejski, G., & Marshall, H., 2000, *ApJ*, in press (astro-ph/9907114)
- Done, C., & Krolik, J. H., 1996, *ApJ*, 463, 144
- Edelson, R. A., & Krolik, J. H., 1988, *ApJ*, 333, 646
- Edelson, R. A., & Nandra, K., 1999, *ApJ*, 514, 682
- Herrero, A., Kudritzki, R. P., Gabler, R., Vilchez, J. M., & Gabler, A., 1995, *A&A*, 297, 556
- Iwasawa, K., et al., 1996, *MNRAS*, 282, 1038
- Iwasawa, K., Fabian, A. C., Young, A. J., Inoue, H., & Matsumoto, C., 1999, *MNRAS*, submitted (astro-ph/9904078)
- Lee, J. C., Fabian, A. C., Reynolds, C. S., Iwasawa, K., & Brandt, W. N., 1998, *MNRAS*, 300, 583
- Levine, A. M., Bradt, H., Cui, W., Jernigan, J. G., Morgan, E. H., Remillard, R., Shirey, R. E., & Smith, D. A., 1996, *ApJ*, 469, L33
- Lomb, N. R., 1976, *Ap&SS*, 39, 447
- McHardy, I.M., 1988. *Memorie della Societa Astronomica Italiana*, 59, 239. ed. Pallavicini, R. and White, N.E.
- McHardy, I. M., Papadakis, I. E., & Uttley, P., 1998, in *The Active X-Ray Sky: Results from Beppo-SAX and RXTE*, ed. L. Scarsi, H. Bradt, P. Giommi, F. Fiore, (Amsterdam: Elsevier), 509, in press
- Miyamoto, S., Kimura, K., Kitamoto, S., Dotani, T., & Ebisawa, K., 1991, *ApJ*, 383, 784
- Miyamoto, S., Kitamoto, S., Mitsuda, K., & Dotani, T., 1988, *Nature*, 336, 450
- Nowak, M. A., 1994, *ApJ*, 422, 688
- Nowak, M. A., Vaughan, B. A., Wilms, J., Dove, J., & Begelman, M. C., 1999, *ApJ*, 510, 874
- Peterson, B. M., & Wandel, A., 1999, *ApJ*, 521, L95
- Peterson, B. M., Wanders, I., Horne, K., Collier, S., Alexander, T., Kaspi, S., & Maoz, D., 1998, *PASP*, 110, 660
- Reynolds, C. S., & Begelman, M. C., 1997, *ApJ*, 488, 109
- Reynolds, C. S., Fabian, A. C., Nandra, K., Inoue, H., H.Kunieda & K.Iwasawa 1995, *MNRAS*, 277, 901
- Reynolds, C. S., Ward, M. J., Fabian, A. C., & Celotti, A., 1997, *MNRAS*, 291, 403
- Reynolds, C. S., Young, A. J., Begelman, M. C., & Fabian, A. C., 1999, *ApJ*, 514, 164
- Scargle, J. D., 1982, *ApJ*, 263, 835
- Tanaka, Y., et al., 1995, *Nature*, 375
- Yaqoob, T., 1997, *ApJ*, 479, 184
- Young, A. J., & Reynolds, C. S., 2000, *ApJ*, in press (astro-ph/9910168)